CHEMICAL ENGINEERING TRANSACTIONS
VOL. 80, 2020
A publication of AIDIC
The Italian Association of Chemical Engineering
Online at www.cetjournal.it
Guest Editors: Eliseo Maria Ranzi, Rubens Maciel Filho

ISBN 978-88-95608-78-5; **ISSN** 2283-9216
DOI: 10.3303/CET2080015

Biomass Gasification in a Downdraft Gasifier with *in-situ* CO_2 Capture: a Pyrolysis, Oxidation and Reduction Staged Model

Elena Catalanotti*, Richard T.J. Porter, Mazaher Molaei Chalchooghi, Haroun Mahgerefteh

Department of Chemical Engineering, University College London, Torrington Place, London WC1E 7JE, UK
e.catalanotti@ucl.ac.uk

Biomass gasification with *in-situ* CO_2 capture, using calcium oxide as sorbent, has attracted increasing interest as a renewable source of high value products through the production of H_2 rich syngas, while simultaneously presenting considerable potential for mitigating global warming by reducing CO_2 emissions. Many factors influence the final composition of the syngas, such as type and amount of gasifying agent and residence time. Kinetic models play an important role in identifying the specific conditions for controlling the yield and composition of the product gas. When *in-situ* CO_2 capture is used, accurate characterisation of the adsorption reactions in the kinetic scheme is essential for accurate prediction of the H_2 rich syngas composition and the overall assessment of the technology. In this work, a kinetic model for biomass gasification with *in-situ* CO_2 capture in a downdraft gasifier is developed. The model is divided into thermochemical stages of pyrolysis, oxidation and reduction in which gasification in a downdraft gasifier occurs, characterised by different compositions and temperature gradients. The model extends the kinetics to the oxidation zone and includes a mechanism for tar oxidation. Given downdraft gasifier designs, a simplification is made where the kinetic behaviour in each of the different stages is modelled separately and in series by a unique set of reactions. The model is validated against two sets of experimental data and different scenarios of equivalence ratio, steam-to-biomass ratio and sorbent-to-biomass ratio are analysed. Sensitivity analysis show that, employing carbon capture, H_2 yields can increase of up to 50% under selected conditions. The study aims to provide a better understanding of biomass gasification kinetics and to aid the design and operation of downdraft gasifiers.

1. Introduction

Biomass gasification is a widely used process to produce valuable products as an alternative to their production from fossil fuel routes (Boerrigter & Rauch, 2005). The syngas produced can have a variety of useful applications in both the chemical and energy sectors and is considered an important route for producing 'green' H_2. Overall CO_2 emissions from biomass utilisation is considered to be vastly reduced compared to fossil fuels, since growing biomass removes as much from CO_2 from the air as can be emitted when used. The addition of CO_2 capture and storage to the gasification process further reduces the emission rate, making the whole process 'carbon negative', meaning that a net reduction of atmospheric CO_2 can be contributed (Bennetta et al. 2019). Kinetic studies of the reactions involved in the gasification process have been carried out for many decades in order to optimise the conditions and improve efficiency of the overall process, including a customisable simulation package developed by Cabianca et al. (2016).

Figure 1 shows a schematic of a typical downdraft gasifier, where the biomass is fed from the top, the oxidising agent is injected in the centre (oxidation zone), and the produced gas (the syngas) is collected from the bottom. This layout creates a temperature distribution within the reactor where different zones are characterised by different compositions and different chemical reactions occurring in each. Given the high temperatures reached within the reactor, as the biomass is fed in the gasifier, the moisture contained in the feedstock evaporates (drying step). The three main thermochemical steps of pyrolysis, oxidation and reduction follow (Reed et al., 1988). In the pyrolysis zone, the feedstock is converted to char and volatiles, which are partially cracked into CH_4. In the oxidation zone, the volatiles partially react with O_2 to produce CO_2 and H_2O

Paper Received: 2 December 2019; Revised: 16 January 2020; Accepted: 17 April 2020
Please cite this article as: Catalanotti E., Porter R.T., Chalchooghi M.M., Mahgarefteh H., 2020, Biomass Gasification in a Downdraft Gasifier with In-situ CO2 Capture: a Pyrolysis, Oxidation and Reduction Staged Model, Chemical Engineering Transactions, 80, 85-90 DOI:10.3303/CET2080015

through exothermic reactions. In the reduction zone, the products generated from the previous steps (Char, CO_2, CH_4, H_2O) are converted into high energy, combustible gases H_2 and CO through a series of endothermic reactions.

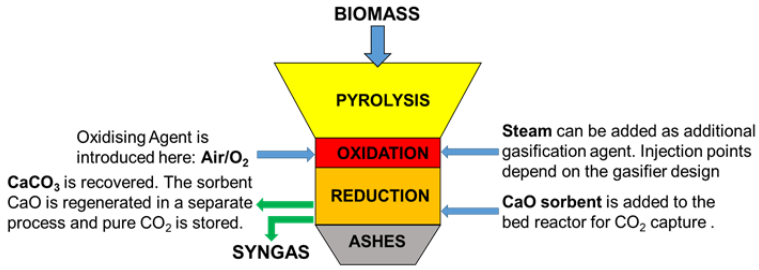

Figure 1: Schematic of a downdraft gasifier showing the different zones within the reactor.

From the point of view of kinetics, pyrolysis and oxidation are the fastest processes, therefore one approach is to assume these processes happen instantaneously and then only model the kinetics of char reduction (Reed, T. B., 1981). The main reactions occurring in the reduction zone are:

1. $C + CO_2 = 2CO$	Boudouard Reaction	4. $CH_4 + H_2O = CO + 3H_2$	Steam-Methane Reforming
2. $C + H_2O = CO + H_2$	Water-Gas Reaction	5. $CO + H_2O = CO_2 + H_2$	Water-Gas-Shift Reaction
3. $C + 2H_2 = CH_4$	Methanation Reaction		

where reactions 1-3 are gas-solid heterogeneous, and 4 and 5 are gas-phase homogeneous.
This approach was chosen by several researchers such as Wang and Kinoshita (1993). Other researchers used a similar approach, but increased the rates proposed by Wang and Kinoshita by introducing a Char Reactivity Factor (CRF) either as a fixed parameter (Giltrap et.al., 2003) or a variable parameter (Babu et.al., 2006). These schemes used stoichiometric assumptions to calculate the distribution of the products generated from pyrolysis and oxidation, considering that all the H_2 and CO generated from pyrolysis would be converted into H_2O and CO_2, and did not include prediction of contaminant species such as tar, which is one of the pyrolysis products. Tar is typically oxidised in the oxidation zone, so in order to evaluate gasification performances and tar production in different conditions, for example with different oxidising agents or equivalent ratios, a kinetic mechanism for the oxidation zone, including tar oxidation, is needed.
Based on the layout of downdraft gasifiers, a mechanism that is divided sequentially into three distinct reaction regimes is proposed in this study, as illustrated in Figure 1. The computed product composition in the pyrolysis zone is used as input concentration together with the addition of pure oxygen or air, in various equivalent ratios (ER), for computing the rate of concentration change in the oxidation zone. The products of the oxidation zone entering the reduction zone, were used as initial concentration for the reduction mechanism.

2. The Model

Biomass can be chemically represented with a general formula of $CH_\alpha O_\beta$, with α = 1.4 and β = 0.56 as an average for wood (Reed & Das, 1988). Char is mainly made of carbon. Tar is a complex mixture of aromatic compounds in various compositions, modelled, in this work, as a mixture of benzene and naphthalene 30:70 wt% (Sreejith et.al., 2015). The reaction rates can be calculated as a function of the rate constant, which follows the general Arrhenius expression in Eq. (1):

$$k = A \exp\left(-\frac{Ea}{RT}\right) \tag{1}$$

Where *k* is the rate constant, *A* is the exponential factor, E_a is the activation energy, *R* is the universal gas constant and *T* is the temperature at which the reaction occurs, which is unique to each zone of the gasifier. The overall rate of each reaction then strictly depends on the concentrations of the species involved. The values of *A* and E_a used are reported in Tables 2 and 3, along with the expressions employed in this work.

2.1 Pyrolysis

Pyrolysis is considered instantaneous, and the distribution of the products is generated using a set of empirical equations (Gomez Barea et al. 2010), based on polynomial expressions with a temperature dependence:

$$f(T) = a_0 + a_1 \frac{T_{pyr}}{T_{ref}} + a_2 \left(\frac{T_{pyr}}{T_{ref}}\right)^2 \tag{2}$$

where a_0, a_1 and a_2 are polynomial coefficients, listed in Table 1, T_{ref} is the reference temperature, an empirical parameter set at 500 °C by Gomez Barea et al. (2010), and T_{pyr} is the pyrolysis temperature in ^{0}C, that can be controlled and adjusted in order to obtain different species compositions in the pyrolysis zone.

Table 1: Polynomial coefficients for the calculation of pyrolysis zone output for a wood feedstock (Gomez Barea et al.; 2010). The yields of char, tar and total gas are expressed in wt % over dry biomass.

	Char wt %	Tar wt %	Gas wt %	CO vol %	CO_2 vol %	H_2 vol %	CH_4 vol %
a_0	-15.03	-196.07	311.10	240.53	-206.86	234.97	-168.64
a_1	50.58	300.86	-351.45	-225.12	267.66	-257.01	214.47
a_2	-18.09	103.34	121.43	67.50	-77.50	72.50	-62.51

The final composition includes water, calculated as the sum of biomass moisture and additional steam based on the Steam-to-Biomass Ratio (SBR) by mass.

2.2 Oxidation

The composition computed in the pyrolysis zone, is used as input for the oxidation calculations along with oxygen or air added based on a specified Equivalence Ratio (ER), defined as the ratio between the oxygen used and the stoichiometric oxygen needed for complete combustion of the biomass, as shown in Figure 1. The temperature of the oxidation zone is fixed at 1000 °C, following from Senelwa (1997). The oxidation scheme was developed by Gerun et al. (2008), with the exception of the WGS, which has been omitted in the present mechanism because it was found to be uninfluential due to the short residence time spent by the gas in the oxidation zone. The expressions are reported in Table 2, along with the parameters of the kinetic constants k_j^{oxi}.

Table 2: Set of reactions used in the oxidation zone (Gerun et al.; 2008)

Reaction	Rate expression	*A*	E_a (J/mol)
1. CO + 0.5 O_2 → CO_2	$k_1^{oxi} cH_2O^{0.5} cCO cO_2^{0.5}$	1.30x10^{11}	1.256×10^{8}
2. CH_4 + 1.5O_2 → CO + 2H_2O	$k_2^{oxi} cCH_4{}^{0.5} cO_2^{1.25}$	4.40x10^{11}	1.255x10^{8}
3. H_2 + 0.5O_2 → H_2O	$k_3^{oxi} cH_2 cO_2$	4.46x10^{12}	4.200x10^{7}
4. C_6H_6 + 4.5O_2 → 6CO + 3H_2O	$k_4^{oxi} cC_6H_6 cO_2^{1.85}$	2.40x10^{11}	1.255x10^{8}
5. $C_{10}H_{18}$ + 7O_2 → 10CO + 4H_2O	$T_{oxi} k_5^{oxi} cC_{10}H_8{}^{0.5} cO_2$	9.20x10^{6}	8.000x10^{7}

2.3 Reduction

The compositions computed in the previous oxidation zone are used as the input concentrations for the reduction zone. Here CaO, the sorbent for CO2 capture, is also added to the composition, according to the variable Sorbent-to-Biomass ratio (SOBR). As the oxidation products move into the reduction zone, the temperature decreases. The typical average temperature in this zone can vary between 800 to 1000 °C (Reed, 1981). The set of reactions and their rate expressions used in the reduction zone are listed in Table 3.

Table 3: Set of reactions and rate parameters used in the reduction zone

Reaction	Expression	*f*	*A*	E_a (J/mol)	Ref.
1. Char + CO_2 ⇋ 2CO	$f_1\ \varepsilon_{ads}\ k_1^{red} cC_{act}(cCO_2 - \frac{cCO^2}{k_{eq,1}})$	10	3.62x10^{1}	7.74x10^{1}	Wang and Kinoshita (1993)
2. Char + H_2O ⇋ CO + H_2	$f_2\ \varepsilon_{ads}\ k_2^{red} cC_{act}(cCO_2 - \frac{cCO cH_2}{k_{eq,2}})$	100	1.52x10^{1}	1.21x10^{2}	Wang and Kinoshita (1993)
3. Char + 2H_2 ⇋ CH_4	$f_3\ \varepsilon_{ads}\ k_3^{red} cC_{act}(cH_2{}^2 - \frac{cCO_2}{k_{eq,2}})$	100	4.19x10^{-3}	1.92x10^{1}	Wang & Kinoshita (1993)
4. CH_4 + H_2O ⇋ CO + 3H_2	$k_4^{red} cCH_4{}^{1.7} cH_2^{-0.8}$	-	3.3x10^{10}	2.4x10^{5}	Sreejit et al. (2015)
5. CO + H_2O ⇋ CO_2 + H_2	$k_5^{red}(cH_2O\ cCO + \frac{cCO_2 cH_2}{k_{eq,5}})$	-	2.8x10^{-2}	6.7x10^{3}	Gao et al. (2008)
6. CaO + CO_2 ⇋ $CaCO_3$	$k_6^{red} cCaO cCO_2$	-	1.02x10^{1}	4.45x10^{1}	Inayat et al. (2010)

The first three reactions are heterogeneous in which the concentration of the solid (mol/m2) corresponds to the availability of reacting sites on the solid, and it is highly dependent of the material and its characteristics of porosity (Golovina, 2002), density, size of particles etc. Since the solid substrate (char) reacts with a gas, and different gases are co-present in the reactor, competitive adsorptions must also be taken into account for each rate expression.

A Langmuir-Hinshelwood mechanism is a valid representation of the adsorption/desorption phenomena occurring during gasification.It reduces the rate by including an adsorption factor ε_{ads} in Eq (3):

$$\varepsilon_{ads} = \frac{1}{(1 + \sum K_{ads,i} * C_i)} \quad (3)$$

where C_i is the concentration of species *i* and $K_{ads,i}$ is the adsorption constant for species *i*. The K_{ads} for the various species were taken from the literature (Karlström et al.; 2015). In the work of Wang & Kinoshita (1993), Arrhenius parameters were obtained by data fitting, therefore the values of the rate constants are strictly dependent on the set of reactions used in the regression as well as to the inlet compositions. As in this work a different set of reactions and inlet conditions are used, the apparent rates were modified by a multiplying factor *f* to obtain a better fit to the experiments.

3. Results

3.1 Model validation

Figures 2a and 2b show the comparison between the model and the experimental data of the gasification of woody biomass in a downdraft gasifier. Experimental data are from Wang and Kinoshita (1994), obtained in pure oxygen conditions, and Chee (1987) in air. Table 4 list the main parameters used in the simulations.

Table 4: List of model-set parameters used for comparison with experimental data.

	Model (Figure a)	Wang & Kinoshita	Model (Figure b)	Chen et al.
Biomass Flowrate (kg/h)	24.7	24.7 (1 mole)	74	74
Residence time (s)	Variable	Variable	5	Not Stated
Reactor Pressure (atm)	1	1	1	1
Moisture (wt%, dry basis)	1%	0	10%	10%
T_{pyr} (°C)	700	Not Stated	700	Not Stated
T_{oxi} (°C)	1000	Not Stated	1275	Not Stated
T_{red} (°C)	800	800	800	Not Stated
ER	0.3	0.3	0.275	0.275
SBR	0	0	0	0
SOBR	0	0	0	0
Char density ρ (kg/m^3)	200	Not Stated	200	192

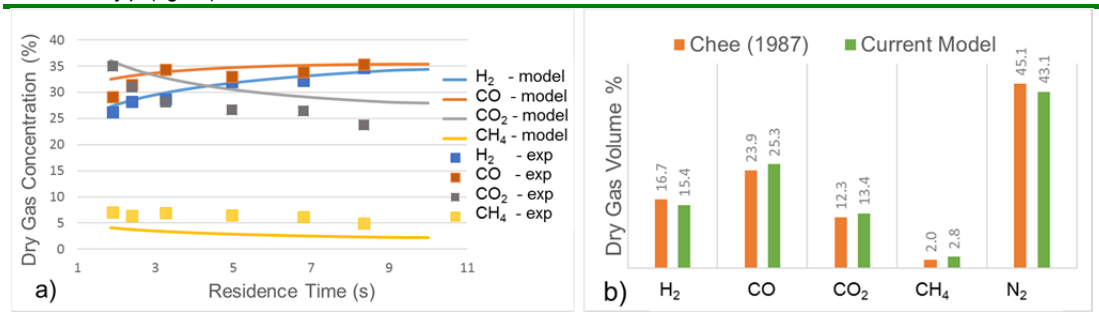

Figure 2: Composition of dry product gas. Comparison of model predictions and experimental data produced from: a) gasification with O_2 at different residence times; b) gasification with air.

The results show reasonable agreement with experiments, although the concentration of CH_4 is slightly under-predicted when pure oxygen is used. CO_2 is instead over-predicted. This suggests that lower rates of combustion of CH_4 are needed to achieve improved estimates. Figure 2b, showing the comparison of predicted dry gas composition at the gasifier outlet to the data of Chee (1987), demonstrates a minor over-prediction of produced gas components in relation to N_2. Typical values for air gasification are found to be around 45-50 vol% N_2. The likely reason is that in air gasification less char is converted into gas than the model predicts. A further test was carried out to assess the behaviour of the mechanism towards tar oxidation. For this test, the initial composition of the gas was changed to that reported by Su et al. (2011) in their experiments and it is shown in Table 5. Figure 3 shows the comparison of the model prediction with the experimental data at different ER. The results were computed until full consumption of O_2 and the residence times were of the order of the milliseconds. According to the results, the model reflects the trend but overestimates the amount of tar still present after oxidation. This could be due to the absence of additional tar

cracking reactions that will also have an impact at temperatures above 1200 °C reached in the oxidation zone or could be due to the influence of inorganic elements in biomass that show catalytic effect on tar cracking(Volpe, R. et al., 2016).

Table 5: Model parameters. Volume and inlet composition as from experiments of Su et al. (2011).

Pres. (atm)	Temp. (°C)	Vol (m^3)	Inlet Composition (kg/h)							
			H_2	CO	H_2O	CO_2	CH_4	Tot Tar	N_2	O_2
1	1000	0.001	0.0008	0.0686	0.8320	0.3187	0.0143	1.0296	0.6828	ER-based

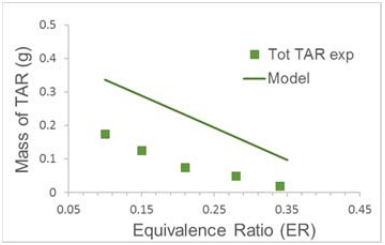

Figure 3: Tar mass in oxidation zone. Model prediction and experimental data from Su et al. (2011).

3.2 Effects of model parameter variance on syngas

Several tests were performed to assess the impact of different parameters such as equivalence ratio, oxidizing agent and sorbent amount, on the produced gas. The model parameters used in these simulations are listed in Table 6 and the results are shown in Figure 4.

Table 6: Model parameters used in sensitivity analyses.

	All runs		Model (Figure 4a)	Model (Figure 5)
Biomass Flowrate (kg/h)	24.7	ER	Variable	0.3
Residence time (s)	5	SBR	0	Variable
Reactor Pressure (atm)	1	SOBR	0	0 and 1
Moisture (wt%, dry basis)	1%			

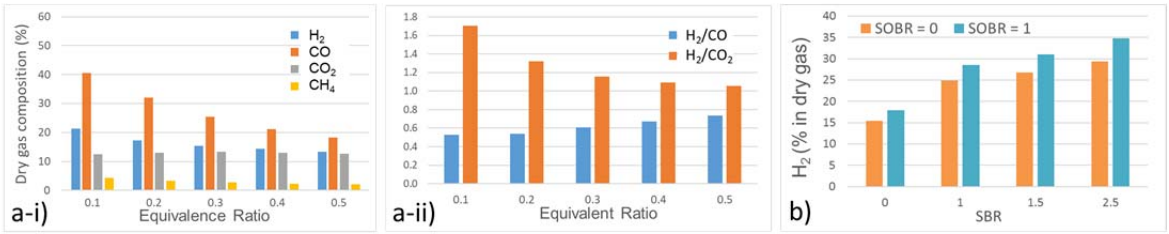

Figure 4: a-i) Dry gas composition obtained at variable ER; a-ii) H_2 to CO and H_2 to CO_2 ratio from the product gas; b) H_2 percentage in dry gas for different SBR gasification conditions, with and without CO_2 capture.

Figure 4a-i shows the composition of the produced gas at different ER in air gasification. As expected, increasing the amount of air has a diluting effect on the amount of gas produced. The composition of the main gases changes as ER increases, with an increase ratio of H_2 to CO, as shown in Figure 4a-ii, meaning that H_2 production is favoured at higher ER. Conversely, CO_2 also increases, due to more oxygen being available in the oxidation zone to combust the CO produced during pyrolysis, with a loss in energy content of the product syngas. For this reason, an optimal value of ER is typically chosen between 0.25 and 0.35.

The addition of steam to the gasification environment strongly favours the production of H_2, as shown in Figure 4b. A change of SBR from 0 to 2.5 almost doubles the amount of hydrogen produced, at a fixed ER of 0.3. This dramatic effect of the steam on H_2 production is due to a combination of factors. Steam is involved in two key reactions in the reduction zone; these are steam gasification (R2; Table 3) and WGS reaction (R5; Table 3), therefore by increasing the amount of steam more char is converted to gas, with formation of H_2, while the presence of extra steam shifts the equilibrium in the WGS reaction towards the production of more H_2. The latter effect is enhanced if sorbent is added to capture the CO_2, as removing CO_2 from the gas-phase further shifts the equilibrium of the WGS reaction towards the production of more H_2. These calculations are strictly dependent on the residence time, with the equilibrium reactions having a bigger impact at longer residence times. Residence time is in turn affected by gasifier design; therefore, the mechanism could

potentially be used to optimise some of the features of the gasifier such as length of the oxidation and of the reduction zones.

4. Conclusions

A kinetic mechanism for the gasification of biomass in a downdraft gasifier has been developed where the three zones of pyrolysis, oxidation and reduction are computed sequentially with unique reaction sets. The mechanism reasonably predicts the concentrations of the main species in the produced gas in both air and oxygen gasification; however, it overpredicts tar concentration, which requires the implementation of a more detailed sub-mechanism. Sensitivity analyses show that H_2 production is favoured at higher ERs and that H_2 yield can be more than doubled by coupling steam gasification and carbon capture with the right gasifier design. Further work is needed to improve the capacity of the model to accurately represent tar production. Plans for future work include introducing cracking reactions, which are expected to occur in the oxidation zone because of the high temperature, as well as investigating tar cracking and reforming in the reduction zone, where the residence time is the longest.

Acknowledgements: This work was supported by a Daphne Jackson Trust Postdoctoral Fellowship, funded by EPSRC and University College London.

References

Babu, B., and Sheth, P. N., 2006, Modeling and simulation of reduction zone of downdraft biomass gasifier: effect of char reactivity factor, Energy Conversion and Management, 47(15-16), 2602-2611.

Bennetta, J., Melara, A., Colosi, L., and Clarens, A., 2019, Life cycle analysis of power cycle configurations in bioenergy with carbon capture and storage, Procedia CIRP 80, 340-345.

Boerrigter, H., and Rauch, R. (2005). In Handbook Biomass Gasification. Biomass Technology Group (BTG).

Cabianca, L., Bassani, A., Amaral, A.F., Rossi, F., Bozzano, G., Ranzi, I., Telen, D, Logist, F., Impeb, J.V., Manenti, F., 2016, GASDS: a Kinetic-Based Package for Biomass and Coal Gasification, Chemical Engineering Transactions, 50, 247-252.

Chee, C. (1987). The air Gasification of wood chips in a downdraft gasifier. PhD Thesis, Kansas City University.

Gao, N., and Li, A., 2008, Modeling and simulation of combined pyrolysis and reduction zone for a downdraft biomass gasifier, Energy Conversion and Management, 49, 3483–3490.

Gerun, L., Paraschiv, M., Vîjeu, R., Bellettre, J., Tazerout, M., Gøbel, B., and Henriksen, U., 2008, Numerical investigation of the partial oxidation in a two-stage downdraft gasifier, Fuel, 87(7), 1383-1393.

Giltrap, D., McKibbin, R., and Barns, G.R.G., 2003, A steady state model of gas-char reactions in a downdraft biomass gasifier, Solar Energy, 74(1), 85-91.

Golovina, E.S., 2002, Investigation of Heterogeneous Combustion and Gasification of Carbon and Solid Fuel (Review), Combustion, Explosion and Shock Waves, 38, 401-408.

Gomez-Barea A., Nilsson, S.; Barrero, F.V. and Campoy, M., 2010, Devolatilization of wood and wastes in fluidized bed, Fuel Processing Technology, 91(11), 1624–1633.

Inayat, A. M., Ahmad, M.M, Yusup, S. and Mutalib, M.I.A., 2010, Biomass steam gasification with in-situ CO2 capture for enriched hydrogen gas production: a reaction kinetics modelling approach, Energies. 3(8).

Karlström, O., BrinK, A., and Huppa, M., 2015, Desorption kinetics of CO in char oxidation and gasification in O2, CO2 and H2O, Combustion and Flame, 162, 788-796.

Reed, T., 1981, Biomass gasification principle and technology. New Jersey: Noyes Data Corporation.

Reed, T., and Das, A., 1988, In Handbook of Biomass Downdraft Gasifier Engine System. SERI, Golden, CO.

Reed, T., and Levie, B., 1988, Fundamentals, development and scale-up of the air-oxygen stratified downdraft gasifier. SERI, PNL-6600.

Senelwa, K., 1997, The air gasification of woody biomass from short rotation forests. New Zeland: Massey University.

Sreejith, C., Muraleedharan, C., and P., Arun, 2015, Air–steam gasification of biomass in fluidized bed with CO2 absorption: A kinetic model for performance prediction Fuel Processing Technology, 130, 197-207.

Su, Y., Luo, Y., Chen, Y., Wu, W., and Zhang, Y., 2011, Experimental and numerical investigation of tar destruction under partial oxidation environment, Fuel Processing Technology, 92(8), 1513–1524.

Volpe, R. Messineo, S., Volpe, M., Messineo, A., 2016, Catalytic effect of char for tar cracking in pyrolysis of citrus wastes, design of a novel experimental set up and first results, Chemical Engineering Transactions, 50, 181-186.

Wang, Y., and Kinoshita, C., 1992, Experimental analysis of biomass gasification with steam and oxygen, Solar Energy, 49, 153-158.

Wang, Y., and Kinoshita, C., 1993, Kinetic model of biomass gasification, Solar Energy, 51(1), 19-24.